

Expression and Function of Kainate Receptors in the Rat Olfactory Bulb

NESTOR G. DAVILA, THOMAS A. HOUP, AND PAUL Q. TROMBLEY*

Department of Biological Science, Program in Neuroscience, Florida State University,
Tallahassee, Florida

KEY WORDS glutamate; RT-PCR; in situ hybridization; electrophysiology; confocal microscopy

ABSTRACT Although recent results suggest roles for NMDA and AMPA receptors in odor encoding, little is known about kainate receptors (KARs) in the olfactory bulb (OB). Molecular, immunological, and electrophysiological techniques were used to provide a functional analysis of KARs in the OB. Reverse transcriptase-polymerase chain reaction revealed that the relative level of expression of KAR subunits was $\text{GluR5} \approx \text{GluR6} \approx \text{KA2} > \text{KA1} \gg \text{GluR7}$. In situ hybridization data imply that mitral/tufted cells express mostly GluR5 and KA2, whereas interneurons express mostly GluR6 and KA2. Immunohistochemical double-labeling experiments (GluR5/6/7 or GluR5 + synapsin) suggest that KARs are expressed at both synaptic and extrasynaptic loci. This heterogeneous expression of KAR subunits suggests that KARs may play a multitude of roles in odor processing, each tailored to the function of specific OB circuits. A functional analysis, using whole-cell electrophysiology, suggests that one such role is to increase the frequency of glutamate transmission while attenuating the amplitude of individual events, likely via a presynaptic depolarizing mechanism. Such effects would be important to odor processing particularly by OB glomeruli. In these highly compartmentalized structures, an increase in the frequency of glutamate release and the high density of extrasynaptic KARs, activated by spillover, could enhance glomerular synchronization and thus the transfer of more specific sensory information to cortical structures. **Synapse 61:320–334, 2007.** © 2007 Wiley-Liss, Inc.

INTRODUCTION

The main olfactory bulb (OB) receives odor information from olfactory sensory neurons in the nasal epithelium, interprets much of that information, and transmits the results to higher cortical regions. Ionotropic glutamate receptors, which mediate the majority of fast excitatory neurotransmission in the nervous system, N-methyl-D-aspartate receptors (NMDARs), α -amino-3-hydroxy-5-methyl-4-isoxazolepropionic acid receptors (AMPA receptors), and kainate receptors (KARs) perform a similar function in the OB. These channels are composed of various combinations of receptor subunits, which confer distinct properties. Autoradiographic data suggest that KARs are highly expressed in the OB (Bailey et al., 2001; Nadi et al., 1980), where immunoreactivity for KAR subunits has been localized to the bulb's principal output neurons (i.e., mitral/tufted [M/T] cells) and interneurons (i.e., periglomerular cells and granule cells) (Montague and Greer, 1999; Petralia et al., 1994). However, it is unclear whether these KARs are functional, localized to synapses, or influence synaptic transmission. In this study, we used a combination of

molecular, immunological, and electrophysiological techniques to provide a functional analysis of KARs in the OB.

KARs are tetramers composed of the glutamate receptor subunits GluR5, GluR6, GluR7, KA1, and KA2 (Lerma et al., 2001), and subunit composition is a key determinant of KAR properties (Contractor et al., 2003; Cui and Mayer, 1999). GluR5, GluR6, and GluR7 can form homomeric receptors or randomly co-assemble with each other and KA1 and KA2, forming functional heteromeric receptors (Cui and Mayer, 1999; Herb et al., 1992; Paternain et al., 2000). Almost every subunit combination results in receptors

Contract grant sponsor: National Institute for Deafness and other Communicative Disorders (National Institutes of Health); Contract grant numbers: DC004320, DC05354-01; Contract grant sponsors: NIA, NICHD, NIDCD, NIDCR, NIGMS, NIMH, NINDS, NINR.

*Correspondence to: Paul Q. Trombley, PhD, Department of Biological Science, Florida State University, Tallahassee, Florida 32306-4340, USA.
E-mail: trombley@neuro.fsu.edu

Received 14 August 2006; Accepted 30 November 2006

DOI 10.1002/syn.20376

Published online in Wiley InterScience (www.interscience.wiley.com).

with distinct kinetic properties and ligand affinities (Cui and Mayer, 1999; Herb et al., 1992; Paternain et al., 2000). Certain subunits also display unique interactions with synapse-associated proteins and second messenger systems e.g., Melyan et al., 2002; Rozas et al., 2003.

The OB is organized into distinct layers. Autoradiographic studies have demonstrated moderate to high levels of KAR ligand binding in the external plexiform layer (EPL) and granule cell layer (GCL) of the mammalian OB, two layers that are rich with synapses (Bailey et al., 2001; Nadi et al., 1980). Using an activity-dependent labeling method, Edwards and Michel showed KAR labeling of ~60–70% of mitral cells, juxtglomerular cells, and granule cells in the zebrafish OB (Edwards and Michel, 2003). In addition to immunological localization of KAR subunits to M/T cells and interneurons (Montague and Greer, 1999; Petralia et al., 1994), *in situ* hybridization (ISH) has shown intense labeling of the KA2 subunit throughout the embryonic OB (Herb et al., 1992). These findings suggest that OB KARs are expressed in proximity to synapses, consistent with the recent demonstration of pre-, peri-, and post-synaptic KARs in other brain regions (Castillo et al., 1997; Chittajallu et al., 1996; Hwang et al., 2001; Kamiya and Ozawa, 2000; Kieval et al., 2001; Rodriguez-Moreno et al., 2000; Vignes and Collingridge, 1997).

Recent electrophysiological data also suggest the presence of functional KARs in the OB, although these studies did not always distinguish between AMPARs and KARs e.g., (Aroniadou-Anderjaska et al., 1999). For example, non-NMDARs (i.e., AMPA and KA receptors) expressed by OB neurons have been shown to take part in LTP (Ennis et al., 1998), calcium-induced calcium release from intracellular stores (Carlson et al., 1997), and even M/T cell self-excitation (Salin et al., 2001; Urban and Sakmann, 2002). In addition, the nonspecific AMPA/KA receptor antagonist, CNQX, or the KA receptor antagonist, LY293558, can prevent the long-lasting depolarization (LLD) that occurs in mitral cells after olfactory nerve stimulation and attributed to glutamate spillover in OB glomeruli (Carlson et al., 2000). More recently, a study employing AMPAR/KAR antagonists (NBQX and SYM2206) showed that somatodendritic excitation of mitral cells depends on fast currents mediated by both AMPARs and KARs as well as slow currents mediated by high-affinity NMDARs (Lowe, 2003).

Taken together, these reports support the notion that OB neurons express functional KARs. As these receptors likely play a role in the processing of olfactory information, we used reverse transcriptase-polymerase chain reaction (RT-PCR), ISH, and immunocytochemistry (ICC) to determine the relative abundance and distribution of KAR subunit mRNAs in the rat OB and whether KARs are expressed at or near

synapses. We also used electrophysiological techniques to test the hypothesis that one functional role for KARs is to modulate glutamatergic-mediated synaptic activity. Our ISH and RT-PCR data reveal that laminar expression patterns and relative amounts of subunit mRNA differ according to KAR subunit. Our ICC data suggest that OB KARs are both synaptic and extrasynaptic and our electrophysiological data suggest that activation of presynaptic KARs modulates glutamatergic transmission among OB neurons. Collectively, these findings suggest that the function of some KARs in the processing of olfactory information is via presynaptic modulation of synaptic transmission, while others may contribute to the effects of glutamate spillover in OB glomeruli.

METHODS

Tissue culture

Preparation of OB primary cultures is described in detail elsewhere (Trombley and Blakemore, 1999). Briefly, OBs were collected from postnatal day 1–5 Sprague-Dawley rat pups. These bulbs were cut into 1 mm³ pieces and enzymatically treated in a calcium/EDTA-buffered papain (Worthington Biochemical, Lakewood, NJ) solution for 1 h at 37°C. Following enzyme inactivation, the tissue was gently triturated with a fire-polished pipette until a single-cell suspension was achieved. The cells (250,000 cells/dish) were plated in 35 mm culture dishes containing a monolayer of previously prepared OB astrocytes. The neuronal media was replaced twice weekly and contained 95% minimal essential medium (Gibco-BRL/Invitrogen, Carlsbad, CA), 5% horse serum (Gibco), 6 g/l glucose, and a nutrient supplement (Serum Extender, Collaborative Research, Bedford, MA). Astrocyte monolayers were obtained by plating a suspension of OB cells in a 75 cm² flask containing 90% minimal essential medium, 10% fetal calf serum, and 6 g/l glucose. The astrocytes were grown to confluence, then resuspended enzymatically with 0.125% trypsin, and plated onto 35 mm dishes coated with poly-L-lysine (30,000–70,000 MW, 10 µg/ml, Sigma-Aldrich, ST. Louis, MO). Cytosine-β-D-arabino-furanoside (10⁻⁵ M) was added to the media one day after plating neurons to prevent the overgrowth of astrocytes. Electrophysiological recordings were made after 7–14 days *in vitro*.

Neuronal identity

M/T and interneurons were identified based on morphological, physiological, and immunohistochemical criteria. Cultures prepared from the OB contained morphologically distinct populations of neurons: a small number of multipolar pyramidal-shaped neurons with large (20–40 µm) somas and a much larger population of small-diameter bipolar neurons (5–10 µm soma).

These morphological characteristics correlate with M/T and granule/periglomerular cells (interneurons), respectively. Electrophysiological analyses further support the notion that they reflect M/T cell and interneurons. Intracellular stimulation of neurons with morphology reflecting M/T cells in vivo invariably evoked glutamate-mediated synaptic events in monosynaptically coupled interneurons. In contrast, intracellular stimulation of the small bipolar neurons evoked GABA-mediated synaptic events, consistent with their identity as interneurons. We also have previously shown that the large pyramidal neurons, the presumptive M/T cells, are *N*-acetylaspartylglutamate immunoreactive; in contrast, the small bipolar neurons, presumptive granule/periglomerular neurons, are glutamic acid decarboxylase immunoreactive (Trombley and Westbrook, 1990).

Electrophysiology

Voltage-clamp and current-clamp recordings were obtained at room temperature (RT). The recording chamber was perfused at 0.5–2.0 ml/min with a solution containing (mM, except glycine, in μ M): NaCl, 162.5; KCl, 2.5; CaCl₂, 2; HEPES, 10; glucose, 10; MgCl₂, 0; and 1 μ M glycine. The osmolarity was 325 mOsm, and the pH was adjusted to 7.3 with NaOH. Patch electrodes were pulled from borosilicate glass and filled with a solution containing (mM): 145 KMeSO₄; 1 MgCl₂; 10 HEPES; 5 Mg-ATP; 0.5 Mg-GTP; and 1.1 EGTA at a pH of 7.2 and an osmolarity of 310 mOsm. Electrode resistances were 4–6 M Ω . Drugs were diluted in the recording solution and delivered by a flow-pipe perfusion system, consisting of an array of eight 400 μ m internal diameter glass barrels fed by gravity from drug reservoirs. The flow pipes were aligned with the neuron using an electronic manipulator and pinch clamps controlled the flow. Patch-clamped neurons were continuously perfused with fast flow from one barrel containing control solution except during the application of drugs. The drugs used here were kainate, glutamate, and SYM2081 ((2*S*,4*R*)-4-methylglutamic acid) (Sigma-Aldrich).

Current signals were recorded with an AxoClamp 2B amplifier (Axon Instruments, Union City, CA), filtered at 1–5 kHz using an eight pole Bessel filter and digitized at 3–15 kHz. Voltage signals were recorded unfiltered. Data was acquired on a G4 Macintosh computer using AxoGraph 4.6 software (Axon Instruments). In all recordings, the membrane voltage and the access resistance were constantly monitored. Data were discarded from cells in which the resting membrane voltage was more positive than -48 mV or the access resistance was ≥ 20 M Ω . No series resistance compensation was used, because the voltage error from the series resistance was ≤ 3 mV for most

recordings. The membrane potentials were corrected for junction potentials, which were usually < 8 mV, for the solutions used. The holding potential was maintained at -65 mV.

Ligand-gated currents were induced in whole cell voltage-clamped neurons via drug perfusion. Spontaneous synaptic activity was recorded from interneurons in current-clamp mode. The event-detection feature in AxoGraph was used to analyze changes in spontaneous synaptic events. Evoked potentials were obtained by simultaneous whole cell recording from monosynaptically coupled M/T cells and interneurons. Positive current injection into the presynaptic M/T cell evoked an action potential, which subsequently induced an evoked excitatory postsynaptic potential (eEPSP) recorded in the postsynaptic interneuron.

Immunocytochemistry and immunohistochemistry

Our ICC procedures were modified from our previous protocols (Davila et al., 2003). Using antisera prepared against GluR5/6/7 (Chemicon, Temecula, CA), GluR5 (Santa Cruz Biotechnology, Santa Cruz, CA), or synapsin (Novagen, Madison, WI), in vitro immunoreactivity was examined in primary cultures of OB neurons 7–14 days after plating. These primary cultures were slowly perfused with 4% formaldehyde in 0.1 M phosphate buffered solution (PBS) before being subjected to the same ICC procedures used for OB slices (see below).

To obtain OB slices, adult Sprague-Dawley rats were anesthetized with inhaled halothane and then transcardially perfused with 100 ml of 0.1 M PBS (pH 7.2) containing 0.2% heparin, followed by 250 ml of a 4% formaldehyde solution. After dissection, the OBs were cryoprotected by overnight immersion in a 30% sucrose solution. Then, the bulbs were rinsed in PBS for 15 min at RT prior to being sectioned into 8–30 μ m coronal slices with a freezing microtome. Slices were mounted onto Superfrost Plus slides (Fisher Scientific, Hampton, NH). An antigen retrieval protocol using Antigen Plus buffer (pH 6.0) was then employed according to the manufacturer's specifications (Novagen, Madison, WI).

Subsequent ICC procedures were similar in OB slices and cultures. Tissues were rinsed three times before incubation in blocking solution consisting of 1% casein in Tris buffered solution (Pierce, Rockford, IL) for 1 h at 4°C. Tissues were then incubated overnight at 4°C in a 1:1000–5000 dilution of the primary antisera in PBS. Primary antibody solutions were removed via aspiration, and tissues were rinsed three times with PBS. Next, tissues were incubated for 2 h at RT in secondary antisera diluted in PBS (1:200–666; Alexa-Fluor 488 labeled goat antimouse IgM, cy-5 labeled rabbit antigoat IgG, or cy-5 labeled donkey

antirabbit IgG (Molecular Probes, Eugene, OR, Sigma-Aldrich, and Jackson Immuno Research Labs, respectively). Tissues were rinsed three times in PBS, and both slice and culture specimens were coverslipped.

To control for nonspecific binding, we conducted parallel immunological experiments, in which 1% casein solution was substituted for the primary antibody. We also controlled for crossreactivity in the double-labeling experiments. Using the same light intensities and optical gain at which we obtained the immunological data, no detectable staining was found in any of our controls.

Cellular expression patterns and colocalization of immunoreactivity were visualized with either a Zeiss 510 Laser Scanning Confocal Microscope (Carl Zeiss, Thornwood, NY) or a Leica DM Light/Fluorescence Microscope (Leica Microsystems, Wetzlar, Germany). A Hamamatsu Orca-ER CCD (Hamamatsu Corporation, Bridgewater, NJ) digitized images were collected on the Leica microscope. We collected and analyzed these images using MetaMorph 5.0 (Universal Imaging Co., Downingtown, PA), OpenLab 3.0 (Improvision Ltd., Lexington, MA) and NIH ImageJ 1.29b software (NIH, Bethesda, MD). Immunoreactivity on confocal images was quantified in overlaid images containing 2–3 sequential 1 μm optical slices. Only pixels brighter than two standard deviations above the mean labeling intensity were considered representative of total immunological labeling. If this labeling from synapsin (green) and KAR subunits (red) overlapped, it was considered “colocalized” for quantification and pseudocolored yellow in the figure.

Quantitative RT-PCR

OBs were quickly frozen after decapitation of halothane anesthetized adult male rats. Total mRNA was reverse transcribed (Ambion, Austin, TX) to obtain the complementary DNA. Briefly, 5 μg of total RNA was added to a solution containing oligo-dT-T₇ (100 ng/ μL) and ddH₂O, incubated for 10 min at 70°C, and then chilled on ice for 5 min. After adding 5 \times first-strand buffer (250 mM Tris-HCl, 375 mM KCl, 15 mM MgCl₂), 0.1 M DTT, dNTPs (10 mM each), RNaseOUT ribonuclease inhibitor, (Invitrogen), and 1 μl Superscript II (RNase H⁻ Reverse Transcriptase, Invitrogen), the reaction was incubated for 3 h at 37°C. A 15-min incubation at 70°C terminated the reverse transcription reaction.

For the PCR, primers were constructed (Genset, LA Jolla, CA) using previously identified oligonucleotide sequences for KAR subunits (Paarmann et al., 2000). Five microliters of a 1:10 dilution of the reverse transcription product, 45 μl of Platinum Supermix (Invitrogen), and 1 μl (10 mM) of each appropriate primer pair were combined for the PCR reaction. PCR cycling

began with an incubation at 94°C for 5 min, followed by 38 amplification cycles at 94°C for 30 s, 60°C for 30 s, then 72°C for 35 s in an automated thermocycler (PTC-200 DNA Engine, MJ Research, Watertown, MA). Between 1 and 5 μl of each PCR product were electrophoresed on a 1.5% agarose gel containing SYBR Gold (Molecular Probes, Eugene, OR). Gels were imaged and the PCR products were quantified using a Kodak Gel Logic 100 and the accompanying Kodak 1D Image Analysis Software (Eastman Kodak Co., Rochester, NY).

We produced a standard curve for each KAR subunit by subjecting 100–0.01 mM of serially diluted plasmids containing one KAR subunit to the same PCR protocol as the OB reverse transcription product in triplicate. The band intensities of the electrophoresed plasmid PCR product were quantitated and plotted for comparison with the PCR product from the OBs. The standard curves for each KAR subunit did not significantly differ, which allowed us to obtain an average value for all of the curves. The amount of PCR product from OBs that was electrophoresed and analyzed was within the dynamic range of the standard curve. The band intensities of PCR products from each OB were normalized for comparison. This procedure provided the relative quantities or ratios of mRNA for each KAR subunit.

In situ hybridization

OBs from male, adult rats were also obtained (as described above) for immunological staining. This tissue was cut into 20–40 μm slices, submerged in cold 2 \times SSC/DEPC, then transferred to prehybridization buffer consisting of denatured salmon sperm, 0.1 M DTT, 20 \times SSC (0.3 M NaCl, 0.03 sodium citrate, pH 7.0), formamide, 5 \times TED (10 mM Tris, 5 mM EDTA/100 mM DTT), and 50 \times Denhardt's for 3 h. Next, we added 10 \times 10⁶ c.p.m. of ³⁵S-labeled complementary DNA probe for each KAR (purified PCR product from plasmids \approx 400 base pairs in length; sequence verified by automated sequence) and incubated the slices for 16 h at 48°C. Then, slices were washed in increasingly stringent concentrations of SSC (from 2 \times to 0.125 \times) and mounted on glass slides in 0.05 M PBS. The slides were exposed to autoradiographic films (Eastman Kodak, Rochester, NY) for 12–72 h to determine the exposure time needed for photoemulsion-dipped slides (1–3 weeks). After developing the photoemulsion-dipped slides, we counterstained them with cresyl violet to facilitate identification of cellular structures. Slices were visualized on an Olympus Provis AX70 (Olympus America, Melville, NY) under darkfield illumination. Relative grayscale values of hybridization (between 0 and 255) were quantitated from darkfield images using a custom image analysis program (MindsEye 1.27b, T. Houpt). In 10 sections

from five rats, densitometry analysis was restricted to hand-drawn outlines of each OB layer. Background values taken from a region near each slice was subtracted from all hybridization values for that slice. Hybridization signals brighter than two standard deviations above the mean optical density were considered representative of total hybridization. ANOVA was used to compare the data corresponding to each KAR subunit across OB layers.

Statistics

Data were compiled in Excel (Microsoft, Redmond, WA), and analyses were performed using Prism 4.00 (GraphPad Software, San Diego, CA). Matched pairs of data were analyzed using the Wilcoxon signed rank test. Statistical significance for RT-PCR data was determined using Friedman analysis. ISH data were transformed by taking the logarithm of each data point, in order to fulfill the assumption of equal variances required for use of ANOVA. All data are presented as the mean \pm SEM. In all figures, statistical significance is denoted as follows: * $P < 0.05$, ** $P < 0.01$, *** $P < 0.005$.

Animal use

All animals were used in accordance with the institutional guidelines of *The Care and Use of Laboratory Animals* approved by the National Institutes of Health and The Florida State University's Animal Care and Use Committee.

RESULTS

Distribution of KARs

Determining whether the KARs expressed on OB neurons in slice and primary culture preparations are synaptic, extrasynaptic, or both provides insight about the physiological function and importance of these receptors. As both the olfactory nerve (which synapses with M/T cell primary dendrites in the glomerular layer [GL]) (Berkowicz et al., 1994; Ennis et al., 1996) and M/T cell primary dendrites release glutamate (Schoppa and Westbrook, 2002; Urban and Sakmann, 2002), KARs localized to M/T cell primary dendrites may function both presynaptically and postsynaptically, whereas extrasynaptic receptors may contribute to the effects of glutamate spillover. In the EPL, KARs localized to M/T cell secondary dendrites may function as autoreceptors and participate in the presynaptic modulation of glutamatergic signals, whereas KARs localized to granule cell spines may be involved in the postsynaptic transduction of glutamatergic signals. In the GCL, KARs may localize presynaptically to M/T cell axons' *boutons en passage* or to postsynaptic sites on the granule cells.

Results from previous immunological (Montague and Greer, 1999; Petralia et al., 1994) and ligand-binding studies (Bailey et al., 2001; Nadi et al., 1980) support all of these possible sites of KAR surface expression in the OB. As a given receptor's anatomic deposition correlates with its function, we performed immunohistochemical labeling of the KAR subunits GluR5/6/7 or GluR5 alone (Fig. 1, in red) and the synapse-specific protein, synapsin (Fig. 1, in green) (Stone et al., 1994), in OB primary cultures and slices.

ICC for GluR5/6/7 and synapsin in OB primary cultures revealed puncta of KAR labeling that colocalized with synapsin labeling (Fig. 1A, yellow, arrowheads); however, many examples of completely segregated staining of these proteins were also evident, suggesting an extrasynaptic population as well. In addition, several interneurons only labeled for synapsin. Further investigation with confocal microscopy revealed slightly different staining patterns in OB slices. GluR5/6/7 labeling was evident in almost every layer of the bulb, particularly in the GL (Fig. 1B) and EPL. The synapsin labeling was similar to previously published data (Stone et al., 1994); however, GluR5/6/7 labeling (Fig. 1B, arrows) primarily appeared to complement rather than colocalize with synapsin labeling (Fig. 1B, arrowheads). Also, mitral and granule cell bodies labeled for GluR5/6/7. These findings obtained with a nonselective antibody (to GluR5/6/7) are in contrast to those obtained with an antibody selective for GluR5. GluR5 labeling more frequently colocalized with synapsin labeling, especially in the GL (Fig. 1C) and GCL, but few puncta were found in the EPL. Although some of the "colocalization" in the slices may, in fact, be the result of superpositioning of closely apposed epitopes, together, our data suggest that GluR5 subunits are found closer to presynaptic proteins than GluR6/7 subunits. A quantitative analysis of the patterns of colocalization supports this interpretation. Only ($4.0 \pm 1.2\%$) of the GluR5/6/7 labeling colocalized with synapsin ($n = 4$ rats, 5 images each). In contrast, ($17.2 \pm 3.1\%$) of the GluR5 labeling colocalized with synapsin ($n = 4$ rats, 5 images each). The difference between these groups was statistically significant ($P < 0.01$). These subcellular distribution patterns may denote different roles for KARs composed of different subunits.

Relative concentrations of OB KAR subunit mRNAs

Because the subunit composition of a given KAR determines its properties (e.g., ligand affinities, kinetics) and pattern of expression, we used RT-PCR to determine the relative concentrations of KAR subunit mRNAs expressed in the OB. Total RNA from OBs was subjected to RT-PCR, and the PCR product

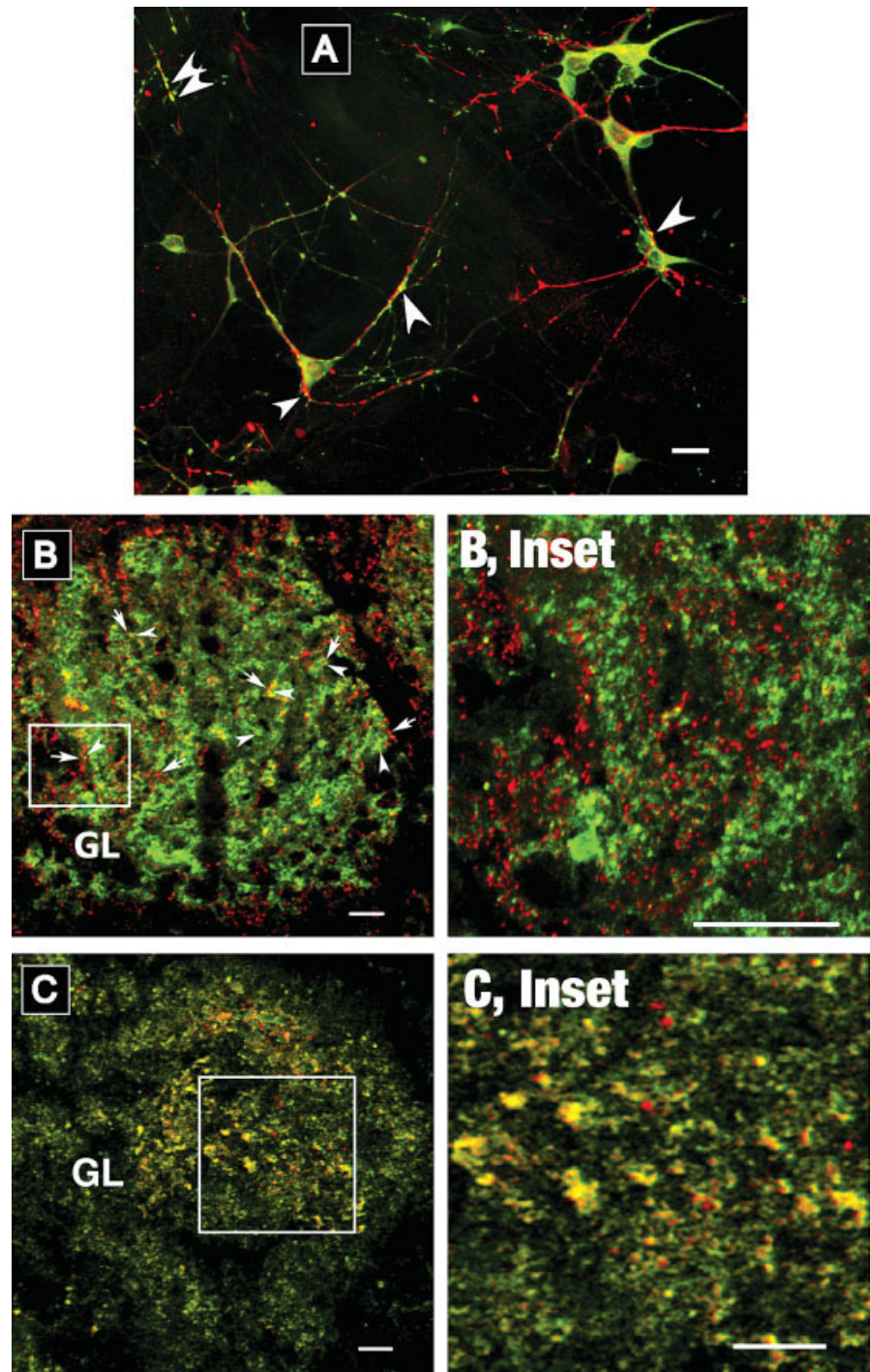


Fig. 1. Immunological labeling of the kainate receptor (KAR) subunits GluR5/6/7 or GluR5 and the synapse-associated protein, synapsin. **A:** Although staining for the KAR subunits GluR5/6/7 (red) and synapsin (green) often colocalized (yellow) in primary culture (see arrowheads), completely segregated patterns of labeling also exist. **B:** ICC performed on OB slices revealed considerable specific staining for both GluR5/6/7 (red, arrows) and synapsin (green, arrowheads). Colocalization of these proteins (yellow) was also apparent in the GL (B and B, Inset), at the GL-EPL interface, and in the EPL, MCL, and GCL (not shown). **C:** Use of a more selective (GluR5-specific) antibody revealed extensive colocalization of synapsin with GluR5 in the GL (C and C, Inset), EPL, MCL, and GCL (not shown). Synapsin-labeling alone (green) far exceeds GluR5-labeling alone (red), with most of the GluR5 labeling colocalized with synapsin. In particular, colocalization is abundant in the GL and the GCL. Scale bar in A is 20 μm ; all others are 10 μm .

was electrophoresed. The resulting band intensity was quantified, normalized, and plotted on a previously developed standard curve (Fig. 2, Top panel) to determine the initial relative quantities of KAR subunit mRNA (Fig. 2, Bottom panel, in mM, $n = 6$). A representative gel is displayed in Figure 2 (Middle panel). Our results suggest that whereas all KAR subunits are transcribed, the other subunits outnumber the GluR7 subunit by $\sim 50:1$. The relative level of

expression of KAR subunits was $\text{GluR5} \approx \text{GluR6} \approx \text{KA2} > \text{KA1} \gg \text{GluR7}$.

Patterns of KAR subunit mRNA expression are distinctly laminar

Although the RT-PCR provided relative levels of mRNA transcribed, these data do not specify in which OB layers these mRNAs are expressed. To address

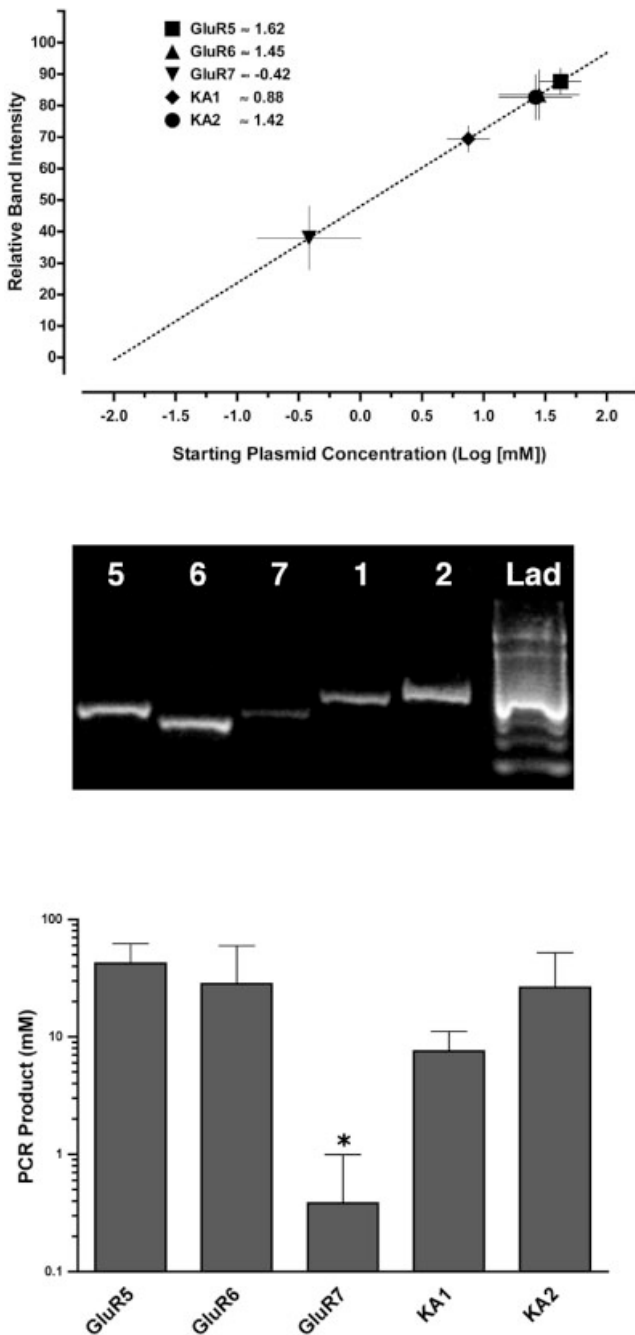


Fig. 2. Concentrations of OB KAR subunit mRNA determined by RT-PCR. Top panel: Relative concentrations of OB KAR subunits were calculated by comparing band intensities of electrophoresed PCR product to this standard curve. Middle panel: Depicted here is a representative gel with SYBR gold-stained PCR products. KAR subunits are designated by their corresponding number only; the last lane is a 500 base pair ladder. Bottom panel: Averages of normalized band intensity data were plotted on the standard curve. The results show significantly more subunit mRNA that was detected for GluR5, GluR6, KA1, and KA2 than GluR7 ($n = 6$, $*P < 0.01$).

this question, we performed ISH and quantified the resultant hybridization patterns (Figs. 3A–3E). To date, only one other study has provided ISH evidence

of any KAR subunit mRNA (KA2, in this example) in the rat OB (Herb et al., 1992); this study also provided evidence against the expression of mRNA for the KA1 subunit.

Our ISH results extend those of Herb et al. (1992) by demonstrating distinct laminar patterns for each of the KAR subunit's mRNAs expressed throughout the OB; this finding suggests that the majority of the hybridization was specific to neurons and not widely distributed among astrocytes or glia (Bailey and Shipley, 1993; Chiu and Greer, 1996). However, the overall density of glia in the OB is low, thus it may be that glia express KARs but that the number of neurons far exceeds the number of glia.

GluR5 hybridization was strongest in the mitral cell layer (MCL) and the abutting internal plexiform layer (IPL), followed by relatively weak staining in the EPL and GL (Fig. 3A). GluR6 hybridization was most intense in the GCL, with moderate labeling in the IPL and GL (Fig. 3B). Interestingly, levels of GluR7 hybridization were weak yet significant in the subependymal zone (SEZ) and EPL (Fig. 3C). No discernible hybridization pattern for the KA1 subunit was found (Fig. 3D). In contrast, significant KA2 labeling was found in every OB layer in which any other KAR probe hybridized (Fig. 3E). Based on these data, we propose that principal cells (mitral cells and probably tufted cells in the EPL) transcribe mostly GluR5 and KA2 mRNA, whereas interneurons (granule cells and periglomerular cells) primarily transcribe GluR6 and KA2 mRNA.

KAR activation increases frequency of glutamate transmission

It is unclear whether KARs on OB neurons influence synaptic transmission. Because application of low concentrations of a KAR agonist has previously been shown to modulate synaptic transmission in the hippocampus (Kamiya and Ozawa, 2000; Lauri et al., 2001a; Schmitz et al., 2001), spinal cord (Kerchner et al., 2002), and cerebellum (Delaney and Jahr, 2002), we monitored changes in the spontaneous activity of current-clamped OB interneurons during KAR activation to test whether KARs mediated similar effects in the OB (Fig. 4). In these experiments, 1 μ M KA was applied to specifically activate kainate, but not AMPA, receptors (Dai et al., 2002; Lerma et al., 1993).

In all interneurons tested, spontaneous excitatory activity increased during KA application. Kainate (1 μ M) increased the frequency of excitatory synaptic events ≥ 5 mV from 0.85 ± 0.39 Hz to 1.91 ± 0.61 Hz (Fig. 4, $n = 9$, $P < 0.05$). In addition, KA application produced EPSPs in 2 cells (one of which was an M/T cell, data not shown) that showed no synaptic activity prior to KA application. These data suggest that KAR

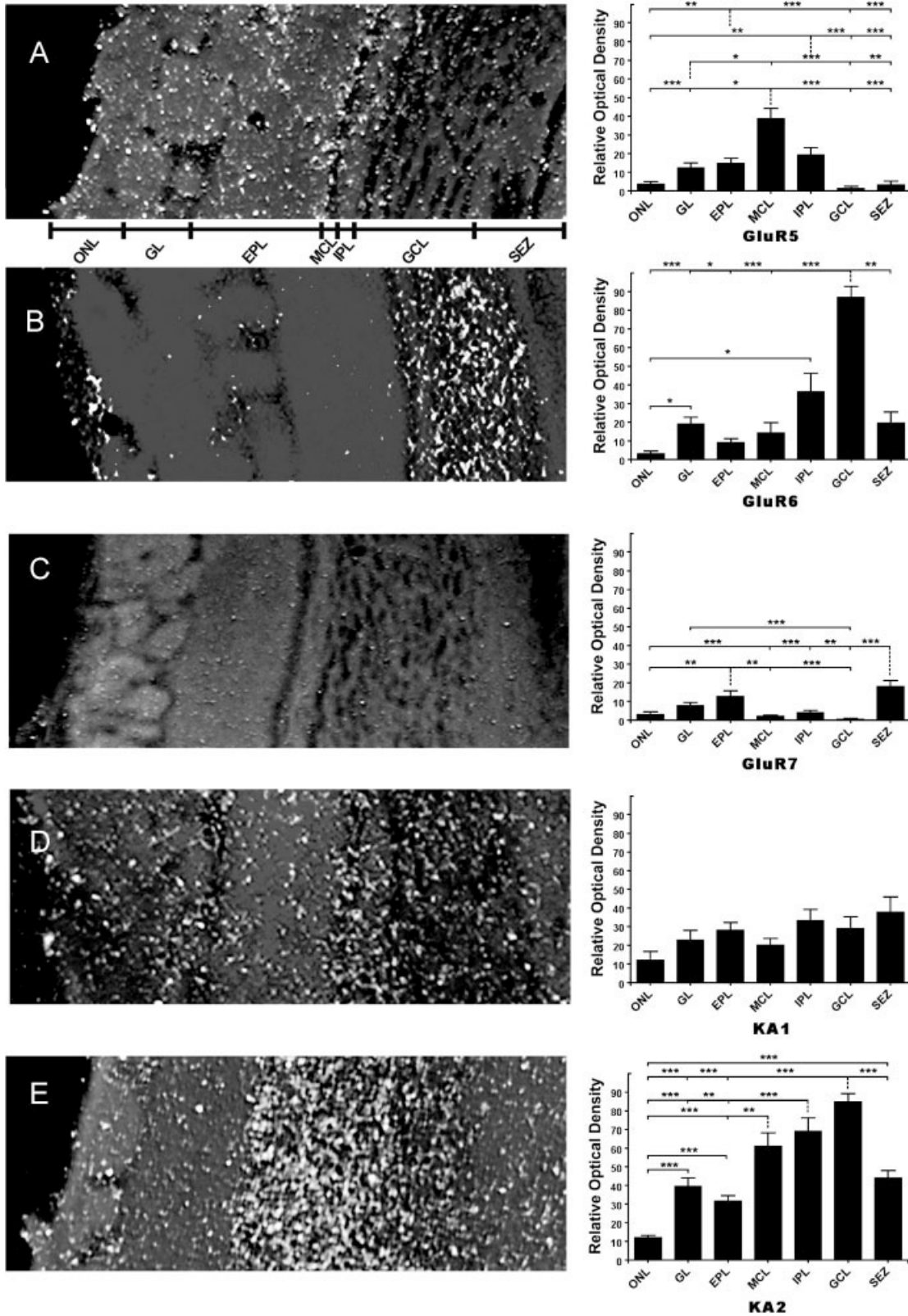


Fig. 3. In situ hybridization (ISH) for KAR subunit mRNA revealed distinct patterns of expression in the OB. A–E: Depicted here are emulsion-dipped OB slices hybridized with radiolabeled probes for GluR5 (A), GluR6 (B), GluR7 (C), KA1 (D), and KA2 (E). Only the brightest 5% of optical signals were considered significant and included for analysis. Accompanying each picture is a histo-

gram (right) of the relative optical density (in %) of hybridization between OB layers. This quantitation allowed determination of statistical differences ($n = 5$). Note the intense hybridization signal for GluR5, GluR6, KA1, and KA2 vs. the relatively weak signal for GluR7 corroborating the RT-PCR analysis above. Statistical significance is denoted by: * $P < 0.05$, ** $P < 0.01$, *** $P < 0.005$.

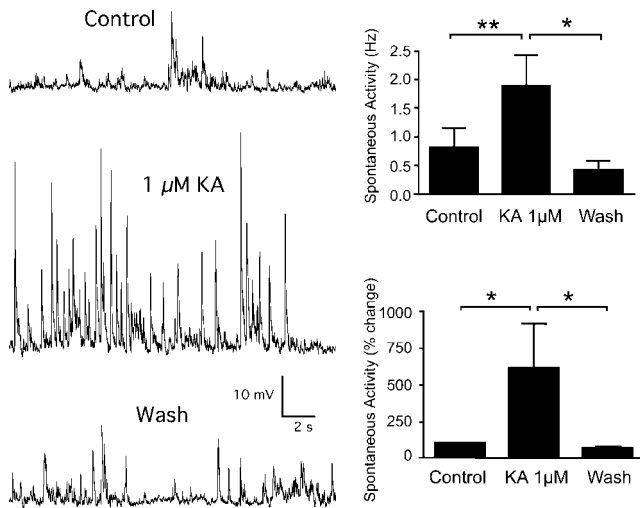


Fig. 4. KAR activation increases interneuronal spontaneous activity. Left panels: Current-clamp traces showing the significant increase in spontaneous activity during 1 μM KA perfusion. Right panels: Histograms of results illustrating the significant increase in interneuronal activity. Excitatory postsynaptic potential (EPSP) frequencies increased from 0.85 ± 0.39 Hz in control solution to 1.91 ± 0.61 Hz in 1 μM KA (Top right), corresponding to a $(609 \pm 318)\%$ change in the normalized spontaneous activity frequency (Bottom right, $n = 9$). Statistical significance is denoted as follows: * $P < 0.05$, ** $P < 0.01$, *** $P < 0.005$.

activation can increase M/T cell-mediated glutamatergic transmission.

KAR activation has no direct effect on postsynaptic membrane properties

To investigate potential postsynaptic effects of KAR activation, we voltage-clamped interneurons at -65 mV and perfused them with a low, modulatory concentration of KA (1 μM); no detectable current was induced (Fig. 5A, $n = 7$).

We also tested the effect of 1 μM KA on membrane resistance. Current-clamped interneurons were injected with a hyperpolarizing current, and the resulting voltage deflection was measured during application of control solution or KA. Kainate (1 μM) did not change the amplitude or kinetics of the deflection (from control) (Figs. 5B₁ and 5B₂, $n = 5$, $P > 0.05$). These results suggest that a low concentration of KA does not directly open or close a significant numbers of ion channels. However, 1 μM KA does produce a small depolarization in interneurons (see next section). Given the high membrane resistance of interneurons, it is possible that 1 μM KA activates sufficient channels to generate a slight depolarization, but still outside the recording limits of our amplifier to detect as a membrane current or a change in membrane resistance. This is in contrast to the effects of higher concentrations (e.g., 100 μM), in which kainate evoked large currents (mostly by activating AMPA

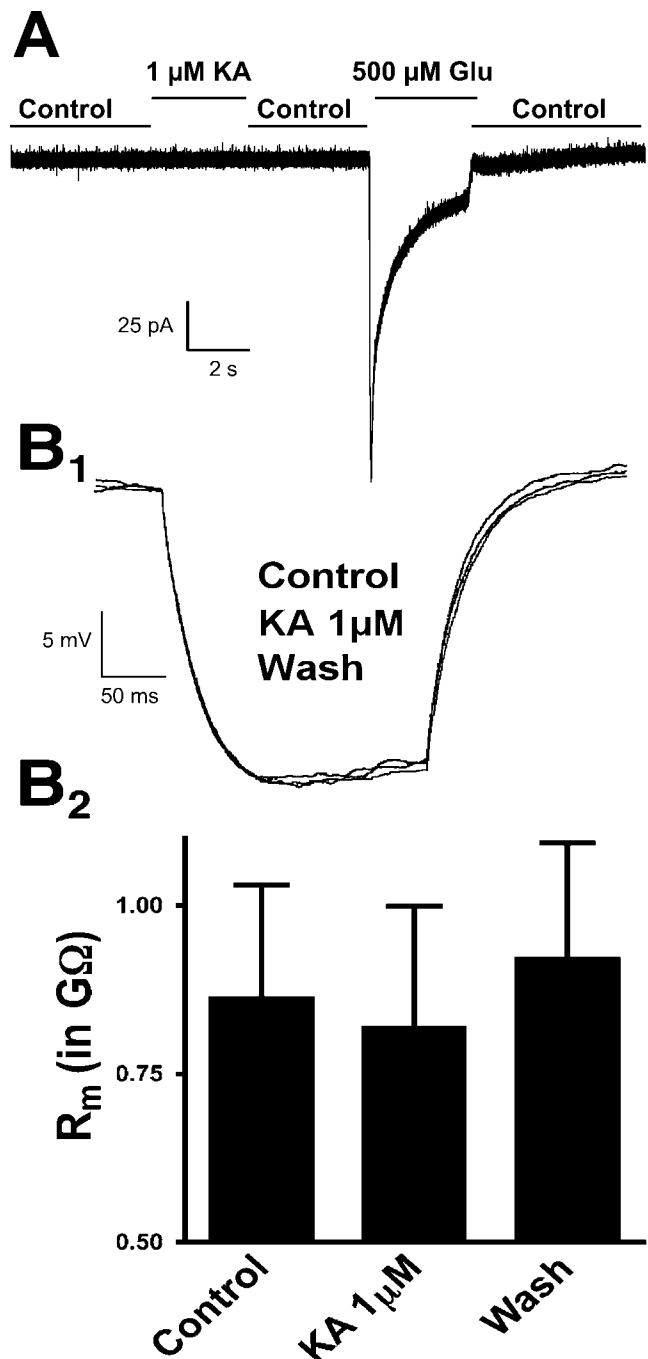


Fig. 5. Perfusing interneurons with a modulatory concentration of KA did not affect postsynaptic membrane properties. A: KA (1 μM) application did not induce a detectable ionotropic current in interneurons (voltage-clamped at -65 mV, $n = 7$). The current induced by glutamate (500 μM) application was included in this trace for comparison. B: Membrane resistances in interneurons remained unchanged during KA application, as seen by these representative voltage deflection traces in response to a 25 pA step (B₁) and the accompanying histogram (B₂). Statistical significance is denoted as follows: * $P < 0.05$, ** $P < 0.01$, *** $P < 0.005$.

receptors). However, application of 10 μM SYM 2081, a selective agonist for KARs, evoked small currents in interneurons as did coapplication of 100 μM kainate

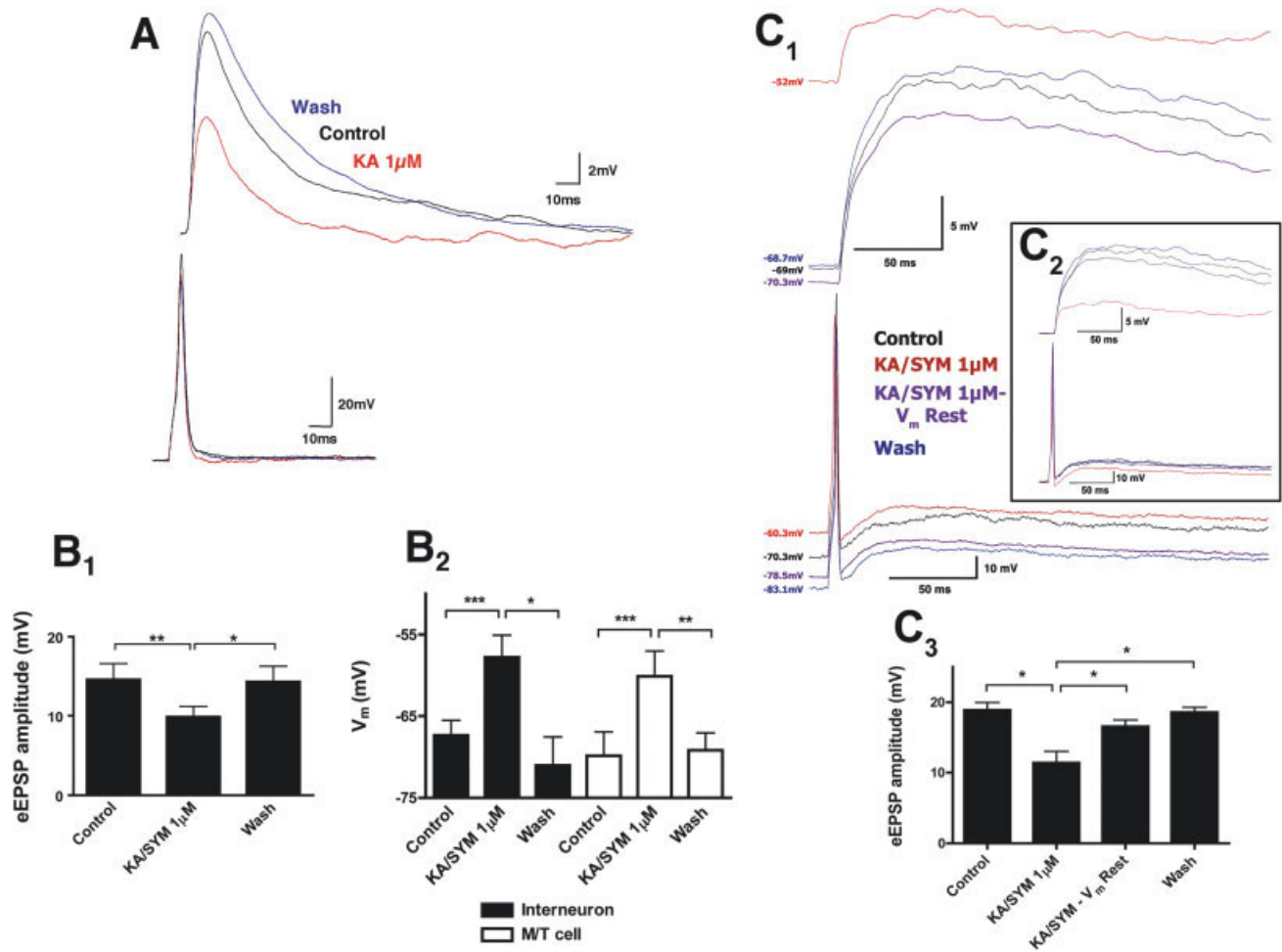


Fig. 6. Perfusion of KAR agonists (KA or SYM2081 [$1 \mu\text{M}$]) attenuated evoked monosynaptic EPSPs via a mechanism involving presynaptic depolarization. **A:** These representative data from a monosynaptically coupled pair of OB neurons illustrates the depressant effect of KAR agonists on eEPSP amplitude (averages of 3 sweeps in each condition). **B:** These graphs summarize the KAR-mediated inhibition of eEPSPs (B_1) and depolarization (B_2) in M/T cells and interneurons (KA and SYM groups combined). **C:** As depicted in

these series of traces (averages of 3 sweeps, C_1), repolarizing only the presynaptic M/T cell to its resting membrane potential during KAR agonist application (KA/SYM $1 \mu\text{M}$ - V_m Rest) prevents the decrease in eEPSP amplitude (C_1 and C_2). The histogram (C_3) summarizes data collected from four pairs of neurons. Note the lack of significant differences between the control, M/T cell repolarization, and wash conditions. Statistical significance is denoted as follows: $*P < 0.05$, $**P < 0.01$, $***P < 0.005$.

and $100 \mu\text{M}$ GYKI 52466 (an AMPA receptor antagonist), indicating the presence of functional KARs.

KAR agonist perfusion attenuates eEPSP amplitude

In interneurons, KAR activation could increase spontaneous activity by presynaptically modulating glutamatergic release, recruiting previously subthreshold glutamatergic inputs, or decreasing GABAergic input onto a given interneuron. To distinguish between these possible monosynaptic and polysynaptic effects, we recorded evoked excitatory synaptic potentials (eEPSPs) from monosynaptically coupled neuron pairs in culture during perfusion of a KAR agonist. Both an M/T cell and interneuron were current-clamped, and a suprathreshold positive current pulse

was injected into the M/T cell to evoke an action potential. The resultant time-locked eEPSP in the interneuron was recorded. The properties and kinetics of the evoked EPSPs were analyzed for changes when KA or SYM2081, a KAR agonist (Zhou et al., 1997), was applied. Figure 6A shows a series of representative traces obtained from a synaptic pair. Perfusion with $1 \mu\text{M}$ of KA or SYM2081 attenuated the amplitude of the eEPSPs (Fig. 6B₁, control, 14.60 ± 2.01 mV; KA/SYM, 9.88 ± 1.34 mV, $n = 8$ pairs, $P < 0.005$). This effect was accompanied by persistent depolarization of both the M/T cell (Fig. 6B₂, control, -69.85 ± 2.93 mV; KA/SYM, -60.10 ± 3.07 mV, $n = 8$ pairs, $P < 0.01$) and interneuron (control, -67.35 ± 1.83 mV; KA/SYM, -57.77 ± 2.69 mV, $n = 8$ pairs, $P < 0.005$).

KAR activation is a known cause of persistent depolarizations in olfactory cortex and hippocampal py-

ramidal neurons (Collingridge et al., 1983; Constanti et al., 1980; Robinson and Deadwyler, 1981; Westbrook and Lothman, 1983). Similar to our findings, recent studies have shown depolarizations and attenuated eEPSPs occurring via activation of presynaptic KARs on mossy fiber terminals. Increased extracellular potassium mimicked the effects of KA, suggesting that these KARs act to depolarize the axons, thereby, initiating at least one presynaptic modulatory mechanism (Schmitz et al., 2001). To test the hypothesis that KARs in the OB function similarly, we hyperpolarized the M/T cell (but not the interneuron) during perfusion with a KAR agonist and analyzed the resultant eEPSPs. Repolarizing the M/T cell to its resting membrane potential occluded the KAR-mediated effect on eEPSPs ($P < 0.05$). The representative traces in Figs. 6C₁ and 6C₂ depict this effect in individual (separated for clarity) and overlaid eEPSPs, respectively. Statistical analyses revealed a significant difference in the amplitudes of the eEPSPs between the 1 μ M KA/SYM group and the other groups (Fig. 6C₃, control, 18.90 ± 1.07 mV; KA/SYM, 11.41 ± 1.63 mV, KA/SYM - V_m Rest, 16.52 ± 0.96 mV, $n = 4$ pairs, $P < 0.05$).

DISCUSSION OB KARs in relation to synapses

Some of the first KAR localization studies in the brain were performed using olfactory-associated brain regions as their model [for review see: (Halasz and Shepherd, 1983)]. For example, Nadi and colleagues provided evidence of distinct KAR ligand-binding in several laminae of the dog OB, particularly in the GCL, MCL, and EPL (Nadi et al., 1980). Later studies supported and extended these autoradiographic data, showing that KAR binding in the OB is comparable with that in the hippocampus, cerebellum, and amygdala (Bailey et al., 2001; Miller et al., 1990; Monaghan and Cotman, 1982; Monaghan et al., 1983, 1985; Unnerstall and Wamsley, 1983).

Immunological evidence to support these ligand-binding studies came recently with the development of nonspecific antibodies to KAR subunits; however, to date, only three studies have used immunological techniques to evaluate KAR distribution in the OB (Montague and Greer, 1999; Petralia et al., 1994; Thukral et al., 1997) and only one focused on OB KARs (Montague and Greer, 1999). Nevertheless, immunological labeling of several KAR subunits in these studies does suggest that they follow specific laminar and cellular distributions (Montague and Greer, 1999; Petralia et al., 1994).

In the present study, we combined immunological techniques with confocal microscopy to show that KARs are localized to synaptic and extrasynaptic sites in the OB. These findings agree with previous studies

and extend those findings by using a more specific KAR subunit antibody (Montague and Greer, 1999; Petralia et al., 1994). Specifically, KARs containing GluR5 seem more likely to be expressed near a given synapse than GluR6/7-containing receptors. Such data suggest that GluR5-containing receptors may participate in fast synaptic transmission, while extrasynaptic GluR6/7-containing KARs may be sensitive to glutamate spillover. Although somata staining in our confocal images from OB slices was not as extensive as that in a previous study (Montague and Greer, 1999), differences in fixation and antigen retrieval techniques, or methods used to visualize binding by the secondary antibodies (i.e., fluorescent detection used here vs. avidin-biotin detection methods used previously), likely explain these findings.

Quantities and patterns of expression of KAR subunit mRNAs

Until now, there has been limited information about where or how much KAR mRNA is expressed in the OB (Herb et al., 1992; van den Pol et al., 1994). In the present study, we found high and specific levels of GluR5 expression in mitral cells and possibly tufted cells. Interestingly, GluR5-containing KARs appear to inhibit glutamate transmission presynaptically at both the mossy fiber-to-CA3 synapse (Lauri et al., 2001b) and Schaeffer collateral-to-CA1 synapse (Clarke and Collingridge, 2002) in the hippocampus. Although our data suggest that KAR activation increases the frequency of glutamate release from M/T cells, its decrease of the amplitude of individual events is consistent with these previous observations.

In contrast to GluR5, GluR6 subunit mRNA was expressed primarily by inhibitory granule and periglomerular cells. Although the function of this subunit remains unclear, GluR6 interacts with the postsynaptic proteins SAP90 and SAP102, which accelerate recovery from desensitization (Bowie et al., 2003) and allow for the subunit's surface expression (Garcia et al., 1998). GluR6 has also been implicated in the modulation of transmitter release e.g., (Contractor et al., 2000). Furthermore, both the GluR5 and GluR6 subunits also have metabotropic properties (Melyan et al., 2002; Rozas et al., 2003).

The SEZ and the EPL both displayed weak but significant hybridization for the GluR7 probe, suggesting that stem cells in the SEZ and a subset of neurons in the EPL (e.g., tufted cells or Van Gehuchten cells) may express this subunit. The lack of KA1-specific hybridization, despite the RT-PCR evidence of significant KA1 transcription, could mean that the KA1 probe failed or that the KA1 mRNA was attributable to glial cells. Another possibility is that KA1 mRNA is evenly distributed across OB layers and cell types, as sup-

ported by the hybridization pattern and our statistical analysis.

The remaining KAR subunit, KA2, exhibited the highest levels of expression and the most extensive hybridization patterns. Functional homomeric receptors cannot be made from KA2 subunits alone (Herb et al., 1992; Ren et al., 2003); hence, these KA2 subunits likely form heteromeric receptors with GluR5 and/or GluR6 on M/T cells and interneurons. As mentioned previously, incorporation of the KA2 subunit can increase ligand affinity and is involved in the presynaptic facilitation of neurotransmitter release (Contractor et al., 2003). KA2 subunits also change the rectification properties of GluR5-containing receptors (Herb et al., 1992), and when coexpressed with GluR6, appear to attenuate the time course and extent of receptor desensitization (Garcia et al., 1998; Herb et al., 1992). In addition, the KA2 subunit appears to be trafficked and regulated differently than GluR5 or GluR6 (Gallyas et al., 2003; Hirbec et al., 2003; Mehta et al., 2001; Ren et al., 2003).

Although the present study provides the most complete analysis of OB KAR subunit expression and heterogeneity, the function of this diversity largely remains unclear. These data set the stage for additional hypotheses about KAR function, but these await the development of more selective subunit-specific agonists and antagonists.

Presynaptic KARs modulate glutamatergic transmission

Recent evidence suggests that somatodendritic excitation of mitral cells depends on fast currents mediated by both AMPARs and KARs as well as slow currents mediated by high-affinity NMDARs (Lowe, 2003). However, the function of KARs in the OB has not been clearly identified. Here, we present electrophysiological data consistent with presence of functional, presynaptic KARs on OB neurons. Application of a low, KAR activating-specific concentration of KA (1 μ M) increased the frequency of excitatory synaptic transmission. This effect was independent of any changes in postsynaptic membrane properties (i.e., application of 1 μ M KA did not induce a change in membrane resistances or holding currents in interneurons). However, KAR activation also diminished the eEPSP amplitude, an effect that was occluded by hyperpolarizing the presynaptic M/T cell back to its resting membrane potential. The reduction in eEPSP amplitude could be due to changes in driving force secondary to the small depolarizations we observed in interneurons (i.e., the membrane potential has moved closer to the reversal potential). Alternatively, the increase in spontaneous activity could lead to a reduction in eEPSP amplitude because of vesicle depletion of the presynaptic neuron. A combination of these effects is also possible.

Although the mechanism by which KAR activation increased the frequency of spontaneous activity remains unclear, our data suggest that depolarization of the presynaptic M/T cell led to the increase. Support for this interpretation comes from similar data collected from where the hippocampal mossy fiber bundle synapses upon CA3 neurons. There, presynaptic KARs depolarize the axons, thereby inducing action potential firing in previously subthreshold axons; concomitantly, the amplitudes of eEPSCs recorded in CA3 neurons decrease (Kamiya and Ozawa, 2000; Schmitz et al., 2001). Similar to our findings, this KAR-mediated effect could be dissociated from any effects on the postsynaptic neuron. Notably, depolarizing the neurons with increased extracellular potassium mimics the KA effect. Our data support the presynaptic depolarization hypothesis, as well as extend these previous observations, by showing that repolarizing the presynaptic neuron (back to its resting membrane potential) occludes the effect of KAR activation.

Our findings also agree with findings in the KAR studies performed on dorsal root ganglion cell axons, or C-fibers, which synapse upon dorsal horn neurons. KAR activation depolarizes the C-fiber afferents and attenuates EPSC amplitudes without altering membrane properties in postsynaptic dorsal horn neurons (Agrawal and Evans, 1986; Kerchner et al., 2001). Together, these data support our conjecture that despite decreasing monosynaptic EPSP amplitudes, KAR activation increases the frequency of glutamate release by depolarizing M/T cells closer to their action potential threshold.

Although our results agree with these previous studies, it is also important to note that these studies (and ours) used sustained (e.g., bath) application of KAR agonists. As the time course of this application does not reflect the time course of activation of these receptors by fast synaptic transmission (or perhaps even the slower activation from spillover), such approaches to drug application may not entirely mimic the consequences of *in vivo* activation of these receptors.

Implications for bulb function and circuitry

The present experiments indicate that kainate receptor (KAR) activation can modulate excitatory transmission by increasing the frequency of glutamate release, but how does this contribute to odor processing by the OB? Although not much is known about KARs in the OB, the present study provides the most complete analysis to date and our data provide some additional insights into KAR function. A recent electron microscopy study showed that OB AMPARs are invariably located at synaptic specializations and that synaptic NMDARs outnumber extrasynaptic NMDARs by \sim 20:1 (Sassoe-Pognetto et al.,

2003). In contrast, our data suggest that KARs are expressed at both synaptic and extrasynaptic regions in the OB, including glomeruli—structures that involve both conventional glutamatergic synaptic transmission as well as glutamate transmission between M/T cell dendrites without identifiable synaptic contacts. In other brain regions, robust extrasynaptic KAR-mediated effects have been seen merely with glutamate spillover (Contractor et al., 2003; Jiang et al., 2001; Li et al., 2001; Schmitz et al., 2003, 2001). Glomeruli appear to be particularly sensitive to spillover because they are highly compartmentalized structures and the concentration of glutamate from spillover is likely enhanced by the ensheathment of primary dendrites by glia (Kasowski et al., 1999). Thus, extrasynaptic OB KARs may participate in glutamatergic signaling induced by glutamate spillover, whereas synaptic OB KARs may contribute to presynaptic modulation and/or fast postsynaptic transduction of glutamatergic transmission.

Olfactory sensory neurons map onto the OB in an odor-specific manner. That is, OSNs expressing receptors for a particular odor map onto one or a few glomeruli (Mombaerts et al., 1996), suggesting that glomeruli act as coordinated units. One prominent characteristic of odor processing by the OB is the synchronization of mitral and tufted cells projecting to an activated glomerulus and the resulting oscillations of activity thought to contribute to odor coding. One mechanism that contributes to such synchronization is lateral excitation within activated glomeruli through glutamate spillover from mitral and tufted cell apical dendrites. Although it appears that electrical coupling via gap junctions may initiate synchronization of M/T cell activity, this activity contributes to spillover, activates AMPA/ KARs, and can lead to further excitation and synchronization within the glomerulus e.g., (Christie et al., 2005; Christie and Westbrook, 2006; Schoppa and Westbrook, 2002).

An additional observation that would support such a role for glomerular KARs is the long-lasting depolarizations (LLDs) thought to play a role in synchronization of intraglomerular M/T cells and attributed to glutamate spillover (Carlson et al., 2000). Olfactory nerve stimulation induces mitral cell LLDs originating in the distal primary dendrite, and recent evidence suggests that KARs may significantly contribute to the current underlying these LLDs (Carlson et al., 2000). For example, the AMPA/KA receptor antagonist CNQX decreased the amplitude of LLDs in a concentration-dependent manner, blocking a quickly developing peak current at low concentrations (relatively AMPA receptor selective) and a slower, longer-lasting current at higher concentrations (blocking both AMPA and KA receptors) (Carlson et al., 2000). Furthermore, application of the kainate receptor antagonist, LY-293558, completely suppressed olfactory

nerve evoked LLDs, strongly implicating KARs in this phenomenon (Carlson et al., 2000). These two constituents of the LLD current also resemble respective AMPAR- and KAR-mediated currents observed in other brain regions (Ali, 2003; Castillo et al., 1997; Cossart et al., 2002, 1998; Dai et al., 2002; Kidd and Isaac, 1999, 2001).

Collectively, these data support the notion that activation of KARs could enhance the synchronous activation of mitral and tufted cells within a glomerulus, via an increase in the frequency of glutamate release, and contribute to the transfer of sensory information from that glomerulus to cortical structures.

ACKNOWLEDGMENTS

The authors thank Dr. Laura Blakemore for her conceptual discussions and assistance with editing of the manuscript.

REFERENCES

- Agrawal SG, Evans RH. 1986. The primary afferent depolarizing action of kainate in the rat. *Br J Pharmacol* 87:345–355.
- Ali AB. 2003. Involvement of post-synaptic kainate receptors during synaptic transmission between unitary connections in rat neocortex. *Eur J Neurosci* 17:2344–2350.
- Aroniadou-Anderjaska V, Ennis M, Shipley MT. 1999. Current-source density analysis in the rat olfactory bulb: Laminar distribution of kainate/AMPA- and NMDA-receptor-mediated currents. *J Neurophysiol* 81:15–28.
- Bailey A, Kelland EE, Thomas A, Biggs J, Crawford D, Kitchen I, Toms NJ. 2001. Regional mapping of low-affinity kainate receptors in mouse brain using [(3)H](2S,4R)-4-methylglutamate autoradiography. *Eur J Pharmacol* 431:305–310.
- Bailey MS, Shipley MT. 1993. Astrocyte subtypes in the rat olfactory bulb: Morphological heterogeneity and differential laminar distribution. *J Comp Neurol* 328:501–526.
- Berkowicz DA, Trombley PQ, Shepherd GM. 1994. Evidence for glutamate as the olfactory receptor cell neurotransmitter. *J Neurophysiol* 71:2557–2561.
- Bowie D, Garcia EP, Marshall J, Traynelis SF, Lange GD. 2003. Allosteric regulation and spatial distribution of kainate receptors bound to ancillary proteins. *J Physiol* 547 (Part 2):373–385.
- Carlson GC, Slawewski ML, Lancaster E, Keller A. 1997. Distribution and activation of intracellular Ca²⁺ stores in cultured olfactory bulb neurons. *J Neurophysiol* 78:2176–2185.
- Carlson GC, Shipley MT, Keller A. 2000. Long-lasting depolarizations in mitral cells of the rat olfactory bulb. *J Neurosci* 20:2011–2021.
- Castillo PE, Malenka RC, Nicoll RA. 1997. Kainate receptors mediate a slow postsynaptic current in hippocampal CA3 neurons. *Nature* 388:182–186.
- Chittajallu R, Vignes M, Dev KK, Barnes JM, Collingridge GL, Henley JM. 1996. Regulation of glutamate release by presynaptic kainate receptors in the hippocampus. *Nature* 379:78–81.
- Chiu K, Greer CA. 1996. Immunocytochemical analyses of astrocyte development in the olfactory bulb. *Brain Res Dev Brain Res* 95:28–37.
- Christie JM, Westbrook GL. 2006. Lateral excitation within the olfactory bulb. *J Neurosci* 26:2269–2277.
- Christie JM, Bark C, Hormuzdi SG, Helbig I, Monyer H, Westbrook GL. 2005. Connexin36 mediates spike synchrony in olfactory bulb glomeruli. *Neuron* 46:761–772.
- Clarke VR, Collingridge GL. 2002. Characterisation of the effects of ATPA, a GLU(K5) receptor selective agonist, on excitatory synaptic transmission in area CA1 of rat hippocampal slices. *Neuropharmacology* 42:889–902.
- Collingridge GL, Kehl SJ, McLennan H. 1983. Excitatory amino acids in synaptic transmission in the Schaffer collateral-commissural pathway of the rat hippocampus. *J Physiol* 334:33–46.
- Constanti A, Connor JD, Galvan M, Nistri A. 1980. Intracellularly-recorded effects of glutamate and aspartate on neurones in the guinea-pig olfactory cortex slice. *Brain Res* 195:403–420.

- Contractor A, Swanson GT, Sailer A, O'Gorman S, Heinemann SF. 2000. Identification of the kainate receptor subunits underlying modulation of excitatory synaptic transmission in the CA3 region of the hippocampus. *J Neurosci* 20:8269–8278.
- Contractor A, Sailer AW, Darstein M, Maron C, Xu J, Swanson GT, Heinemann SF. 2003. Loss of kainate receptor-mediated heterosynaptic facilitation of mossy-fiber synapses in KA2^{-/-} mice. *J Neurosci* 23:422–429.
- Cossart R, Esclapez M, Hirsch JC, Bernard C, Ben-Ari Y. 1998. GluR5 kainate receptor activation in interneurons increases tonic inhibition of pyramidal cells. *Nat Neurosci* 1:470–478.
- Cossart R, Epszstein J, Tyzio R, Becq H, Hirsch J, Ben-Ari Y, Crepel V. 2002. Quantal release of glutamate generates pure kainate and mixed AMPA/kainate EPSCs in hippocampal neurons. *Neuron* 35:147–159.
- Cui C, Mayer ML. 1999. Heteromeric kainate receptors formed by the coassembly of GluR5, GluR6, and GluR7. *J Neurosci* 19:8281–8291.
- Dai WM, Christensen KV, Egebjerg J, Ebert B, Lambert JD. 2002. Correlation of the expression of kainate receptor subtypes to responses evoked in cultured cortical and spinal cord neurones. *Brain Res* 926:94–107.
- Davila NG, Blakemore LJ, Trombley PQ. 2003. Dopamine modulates synaptic transmission between rat olfactory bulb neurons in culture. *J Neurophysiol* 90:395–404.
- Delaney AJ, Jahr CE. 2002. Kainate receptors differentially regulate release at two parallel fiber synapses. *Neuron* 36:475–482.
- Edwards JG, Michel WC. 2003. Pharmacological characterization of ionotropic glutamate receptors in the zebrafish olfactory bulb. *Neuroscience* 122:1037–1047.
- Ennis M, Zimmer LA, Shipley MT. 1996. Olfactory nerve stimulation activates rat mitral cells via NMDA and non-NMDA receptors in vitro. *Neuroreport* 7:989–992.
- Ennis M, Linster C, Aroniadou-Anderjaska V, Ciombor K, Shipley MT. 1998. Glutamate and synaptic plasticity at mammalian primary olfactory synapses. *Ann N Y Acad Sci* 855:457–466.
- Gallyas F, Ball SM, Molnar E. 2003. Assembly and cell surface expression of KA-2 subunit-containing kainate receptors. *J Neurochem* 86:1414–1427.
- Garcia EP, Mehta S, Blair LA, Wells DG, Shang J, Fukushima T, Fallon JR, Garner CC, Marshall J. 1998. SAP90 binds and clusters kainate receptors causing incomplete desensitization. *Neuron* 21:727–739.
- Halasz N, Shepherd GM. 1983. Neurochemistry of the vertebrate olfactory bulb. *Neuroscience* 10:579–619.
- Herb A, Burnashev N, Werner P, Sakmann B, Wisden W, Seeburg PH. 1992. The KA-2 subunit of excitatory amino acid receptors shows widespread expression in brain and forms ion channels with distantly related subunits. *Neuron* 8:775–785.
- Hirbec H, Francis JC, Lauri SE, Braithwaite SP, Coussen F, Mulle C, Dev KK, Coutinho V, Meyer G, Isaac JT, Collingridge GL, Henley JM, Couthino V. 2003. Rapid and differential regulation of AMPA and kainate receptors at hippocampal mossy fibre synapses by PICK1 and GRIP. *Neuron* 37:625–638.
- Hwang SJ, Pagliardini S, Rustioni A, Valtchanoff JG. 2001. Presynaptic kainate receptors in primary afferents to the superficial laminae of the rat spinal cord. *J Comp Neurol* 436:275–289.
- Jiang L, Xu J, Nedergaard M, Kang J. 2001. A kainate receptor increases the efficacy of GABAergic synapses. *Neuron* 30:503–513.
- Kamiya H, Ozawa S. 2000. Kainate receptor-mediated presynaptic inhibition at the mouse hippocampal mossy fibre synapse. *J Physiol* 523 (Part 3):653–665.
- Kasowski HJ, Kim H, Greer CA. 1999. Compartmental organization of the olfactory bulb glomerulus. *J Comp Neurol* 407:261–274.
- Kerchner GA, Wilding TJ, Li P, Zhuo M, Huettner JE. 2001. Presynaptic kainate receptors regulate spinal sensory transmission. *J Neurosci* 21:59–66.
- Kerchner GA, Wilding TJ, Huettner JE, Zhuo M. 2002. Kainate receptor subunits underlying presynaptic regulation of transmitter release in the dorsal horn. *J Neurosci* 22:8010–8017.
- Kidd FL, Isaac JT. 1999. Developmental and activity-dependent regulation of kainate receptors at thalamocortical synapses. *Nature* 400:569–573.
- Kidd FL, Isaac JT. 2001. Kinetics and activation of postsynaptic kainate receptors at thalamocortical synapses: Role of glutamate clearance. *J Neurophysiol* 86:1139–1148.
- Kieval JZ, Hubert GW, Charara A, Pare JF, Smith Y. 2001. Subcellular and subsynaptic localization of presynaptic and postsynaptic kainate receptor subunits in the monkey striatum. *J Neurosci* 21:8746–8757.
- Lauri SE, Bortolotto ZA, Bleakman D, Ornstein PL, Lodge D, Isaac JT, Collingridge GL. 2001a. A critical role of a facilitatory presynaptic kainate receptor in mossy fiber LTP. *Neuron* 32:697–709.
- Lauri SE, Delany C, Clarke VR, Bortolotto ZA, Ornstein PL, J TRI, Collingridge GL. 2001b. Synaptic activation of a presynaptic kainate receptor facilitates AMPA receptor-mediated synaptic transmission at hippocampal mossy fibre synapses. *Neuropharmacology* 41:907–915.
- Lerma J, Paternain AV, Naranjo JR, Mellstrom B. 1993. Functional kainate-selective glutamate receptors in cultured hippocampal neurons. *Proc Natl Acad Sci USA* 90:11688–11692.
- Lerma J, Paternain AV, Rodriguez-Moreno A, Lopez-Garcia JC. 2001. Molecular physiology of kainate receptors. *Physiol Rev* 81:971–998.
- Li H, Chen A, Xing G, Wei ML, Rogawski MA. 2001. Kainate receptor-mediated heterosynaptic facilitation in the amygdala. *Nat Neurosci* 4:612–620.
- Lowe G. 2003. Flash photolysis reveals a diversity of ionotropic glutamate receptors on the mitral cell somatodendritic membrane. *J Neurophysiol* 90:1737–1746.
- Mehta S, Wu H, Garner CC, Marshall J. 2001. Molecular mechanisms regulating the differential association of kainate receptor subunits with SAP90/PSD-95 and SAP97. *J Biol Chem* 276:16092–16099.
- Melyan Z, Wheal HV, Lancaster B. 2002. Metabotropic-mediated kainate receptor regulation of IsAHP and excitability in pyramidal cells. *Neuron* 34:107–114.
- Miller LP, Johnson AE, Gelhard RE, Insel TR. 1990. The ontogeny of excitatory amino acid receptors in the rat forebrain—II. Kainic acid receptors. *Neuroscience* 35:45–51.
- Mombaerts P, Wang F, Dulac C, Chao SK, Nemes A, Mendelsohn M, Edmondson J, Axel R. 1996. Visualizing an olfactory sensory map. *Cell* 87:675–686.
- Monaghan DT, Cotman CW. 1982. The distribution of [³H]kainic acid binding sites in rat CNS as determined by autoradiography. *Brain Res* 252:91–100.
- Monaghan DT, Holets VR, Toy DW, Cotman CW. 1983. Anatomical distributions of four pharmacologically distinct 3H-L-glutamate binding sites. *Nature* 306:176–179.
- Monaghan DT, Yao D, Cotman CW. 1985. L-[³H]Glutamate binds to kainate-, NMDA- and AMPA-sensitive binding sites: An autoradiographic analysis. *Brain Res* 340:378–383.
- Montague AA, Greer CA. 1999. Differential distribution of ionotropic glutamate receptor subunits in the rat olfactory bulb. *J Comp Neurol* 405:233–246.
- Nadi NS, Hirsch JD, Margolis FL. 1980. Laminar distribution of putative neurotransmitter amino acids and ligand binding sites in the dog olfactory bulb. *J Neurochem* 34:138–146.
- Paarmann I, Frermann D, Keller BU, Hollmann M. 2000. Expression of 15 glutamate receptor subunits and various splice variants in tissue slices and single neurons of brainstem nuclei and potential functional implications. *J Neurochem* 74:1335–1345.
- Paternain AV, Herrera MT, Nieto MA, Lerma J. 2000. GluR5 and GluR6 kainate receptor subunits coexist in hippocampal neurons and coassemble to form functional receptors. *J Neurosci* 20:196–205.
- Petralia RS, Wang YX, Wenthold RJ. 1994. Histological and ultrastructural localization of the kainate receptor subunits, KA2 and GluR6/7, in the rat nervous system using selective antipeptide antibodies. *J Comp Neurol* 349:85–110.
- Ren Z, Riley NJ, Garcia EP, Sanders JM, Swanson GT, Marshall J. 2003. Multiple trafficking signals regulate kainate receptor KA2 subunit surface expression. *J Neurosci* 23:6608–6616.
- Robinson JH, Deadwyler SA. 1981. Kainic acid produces depolarization of CA3 pyramidal cells in the vitro hippocampal slice. *Brain Res* 221:117–127.
- Rodriguez-Moreno A, Lopez-Garcia JC, Lerma J. 2000. Two populations of kainate receptors with separate signaling mechanisms in hippocampal interneurons. *Proc Natl Acad Sci USA* 97:1293–1298.
- Rozas JL, Paternain AV, Lerma J. 2003. Noncanonical signaling by ionotropic kainate receptors. *Neuron* 39:543–553.
- Salin PA, Lledo PM, Vincent JD, Charpak S. 2001. Dendritic glutamate autoreceptors modulate signal processing in rat mitral cells. *J Neurophysiol* 85:1275–1282.
- Sassoe-Pognetto M, Utvik JK, Camoletto P, Watanabe M, Stephenson FA, Breddt DS, Ottersen OP. 2003. Organization of postsynaptic density proteins and glutamate receptors in axodendritic and dendrodendritic synapses of the rat olfactory bulb. *J Comp Neurol* 463:237–248.
- Schmitz D, Mellor J, Nicoll RA. 2001. Presynaptic kainate receptor mediation of frequency facilitation at hippocampal mossy fiber synapses. *Science* 291:1972–1976.

- Schmitz D, Mellor J, Breustedt J, Nicoll RA. 2003. Presynaptic kainate receptors impart an associative property to hippocampal mossy fiber long-term potentiation. *Nat Neurosci* 6:1058–1063.
- Schoppa NE, Westbrook GL. 2002. AMPA autoreceptors drive correlated spiking in olfactory bulb glomeruli. *Nat Neurosci* 5:1194–1202.
- Stone LM, Browning MD, Finger TE. 1994. Differential distribution of the synapsins in the rat olfactory bulb. *J Neurosci* 14:301–309.
- Thukral V, Chikaraishi D, Hunter DD, Wang JK. 1997. Expression of non-*N*-methyl-*D*-aspartate glutamate receptor subunits in the olfactory epithelium. *Neuroscience* 79:411–424.
- Trombley PQ, Blakemore LJ. 1999. Mammalian olfactory bulb neurons. In: Haynes LW, editor. *The neuron in tissue culture*. West Sussex, UK: Wiley. p 585–592.
- Trombley PQ, Westbrook GL. 1990. Excitatory synaptic transmission in cultures of rat olfactory bulb. *J Neurophysiol* 64:598–606.
- Unnerstall JR, Wamsley JK. 1983. Autoradiographic localization of high-affinity [³H]kainic acid binding sites in the rat forebrain. *Eur J Pharmacol* 86:361–371.
- Urban NN, Sakmann B. 2002. Reciprocal intraglomerular excitation and intra- and interglomerular lateral inhibition between mouse olfactory bulb mitral cells. *J Physiol* 542 (Part 2):355–367.
- van den Pol A, Hermans-Borgmeyer I, Hofer M, Ghosh P, Heinemann S. 1994. Ionotropic glutamate-receptor gene expression in hypothalamus: Localization of AMPA, kainate, and NMDA receptor RNA with in situ hybridization. *J Comp Neurol* 343:428–444.
- Vignes M, Collingridge GL. 1997. The synaptic activation of kainate receptors. *Nature* 388:179–182.
- Westbrook GL, Lothman EW. 1983. Cellular and synaptic basis of kainic acid-induced hippocampal epileptiform activity. *Brain Res* 273:97–109.
- Zhou LM, Gu ZQ, Costa AM, Yamada KA, Mansson PE, Giordano T, Skolnick P, Jones KA. 1997. (2*S*,4*R*)-4-methylglutamic acid (SYM 2081): A selective, high-affinity ligand for kainate receptors. *J Pharmacol Exp Ther* 280:422–427.